Spontaneous intracerebral hemorrhage during acute and chronic hypertension in mice

Yoshinobu Wakisaka[1], Yi Chu[1], Jordan D Miller[1], Gary A Rosenberg[2] and Donald D Heistad[1,3,4]

[1]Department of Internal Medicine, Cardiovascular Center, University of Iowa, Iowa City, Iowa, USA; [2]Department of Neurology, University of New Mexico Health Sciences Center, Albuquerque, New Mexico, USA; [3]Department of Pharmacology, University of Iowa, Iowa City, Iowa, USA; [4]VA Medical Center, Iowa City, Iowa, USA

Oxidative stress and matrix metalloproteinases (MMPs) contribute to hemorrhagic transformation after ischemic stroke and brain injury after intracerebral hemorrhage (ICH). The goal of this study was to develop a new model of spontaneous ICH, based on the hypothesis that acute, superimposed on chronic, hypertension produces ICH. We hypothesized that increases in angiotensin II (AngII)-mediated oxidative stress and activation of MMPs are associated with, and may precede, spontaneous ICH during hypertension. In C57BL/6 mice, chronic hypertension was produced with AngII infusion and an inhibitor of nitric oxide synthase. During chronic hypertension, mice with acute hypertension from injections of AngII developed ICH. Oxidative stress and MMP levels increased in the brain even before developing ICH. Active MMPs colocalized with a marker of oxidative stress, especially on cerebral vessels that appeared to lead toward regions with ICH. Incidence of ICH and levels of oxidative stress and MMP-9 were greater in mice with acute hypertension produced by AngII than by norepinephrine. In summary, we have developed an experimental model of ICH during hypertension that may facilitate studies in genetically altered mice. We speculate that acute hypertension, especially when induced by AngII, may be critical in spontaneous ICH during chronic hypertension, possibly through oxidative stress and MMP-9.
Journal of Cerebral Blood Flow & Metabolism (2010) 30, 56–69; doi:10.1038/jcbfm.2009.183; published online 2 September 2009

Introduction

Oxidative stress and matrix metalloproteinases (MMPs) may be important in mechanisms of hemorrhagic transformation after ischemic stroke, and in brain injury after intracerebral hemorrhage (ICH) (Gasche et al, 2001; Yang et al, 2007; Zhao et al, 2007; Grossetete and Rosenberg, 2008). Mechanisms that lead to ICH during hypertension, however, remain poorly understood, in part because of a paucity of experimental models of spontaneous ICH in mice (NINDS ICH Workshop Participants, 2005).

Chronic hypertension is a major risk factor for ICH. Recent evidence also suggests that acute hypertension may contribute to ICH (Caplan, 1994; Metoki et al, 2006). Activation of the renin–angiotensin system and sympathetic nerve system is a common mechanism of acute hypertension (Vaughan and Delanty, 2000).

An important mechanism of vascular injury in hypertension is oxidative stress (Heistad, 2006). Angiotensin II (AngII) activates nicotinamide adenine dinucleotide phosphate (NAD(P)H) oxidase and thereby generates high levels of superoxide in cerebral vessels (Didion and Faraci, 2003). We previously developed the first experimental model of spontaneous ICH in hypertensive mice: double transgenic mice with overexpression of human renin and human angiotensinogen (R+/A+), treated with N^{ω}-nitro-L-arginine methyl ester (L-NAME: an inhibitor of nitric oxide synthase) and high-salt diet (Iida et al, 2005; Wakisaka et al, 2008). We found that the increase in superoxide is due, at least in part, to increased activity of NAD(P)H oxidase, which may

contribute to spontaneous ICH in R+/A+ mice (Wakisaka *et al*, 2008).

Several studies suggest that induction and activation of MMPs is redox sensitive (Gasche *et al*, 2001; Liu and Rosenberg, 2005; Rajagopalan *et al*, 1996). Matrix metalloproteinases are a family of zinc endopeptidases that degrade basal lamina and extracellular matrix (ECM) (Woessner, 1991), which may lead to disruption of the blood–brain barrier (Gasche *et al*, 2001; Yang *et al*, 2007). Thus, we speculated that increases in AngII-mediated oxidative stress during chronic, and perhaps acute, hypertension may induce MMPs, and facilitate disruption of the basement membrane, contributing to the pathogenesis of spontaneous ICH.

The first goal of this study was to develop a new model of spontaneous ICH in mice, based on the hypothesis that acute as well as chronic hypertension may produce ICH. Second, we tested the hypothesis that increases in AngII-mediated oxidative stress and activation of MMPs are associated with, and may precede, spontaneous ICH during hypertension. Third, we tested the hypothesis that susceptibility to ICH is greater when acute hypertension is produced by AngII than norepinephrine (NE), because of greater pro-oxidant effects of AngII (Laursen *et al*, 1997).

Materials and methods

Experimental Animals

Studies were conducted on 8-month-old male C57BL/6 mice ($n = 145$; Jackson Laboratories, Bar Harbor, ME, USA). All experimental protocols and procedures conformed to the NIH *Guide for the Care and Use of Laboratory Animals* and were approved by the Institutional Animal Care and Use Committee at the University of Iowa.

There were two cohorts of mice in this study. The first cohort was used to evaluate blood pressure, incidence of stroke, and size of ICH. Mice in this cohort were killed with an injection of Nembutal (150 mg/kg, i.p.) when a mouse developed signs of stroke, or at day 28 if the mouse did not have neurologic signs. The second cohort was used to evaluate oxidative stress, expression of mRNA, and MMPs. In the second cohort, when a mouse developed signs of stroke, the mouse with signs of stroke and one mouse without neurologic signs from each of the other groups were also killed with Nembutal, to collect tissue samples after the same duration of treatment.

Development of the Model of Spontaneous Intracerebral Hemorrhage

Mice were administered an infusion of AngII and L-NAME in drinking water to produce chronic hypertension (chronically hypertensive group). AngII (1,000 ng/kg per min; Sigma-Aldrich, St Louis, MO, USA) dissolved in sterile saline was infused using an osmotic pump (Durect Corporation, Cupertino, CA, USA) that was implanted subcutaneously under anesthesia with ketamine and xylazine (87.5 and 12.5 mg/kg, respectively, i.p.). Treatment with L-NAME (100 mg/kg per day; Sigma-Aldrich) in drinking water was started on the same day of implantation of osmotic pumps. After 1 week acute hypertension was produced in some chronically hypertensive mice by injections of AngII (0.5 μg/g, twice per day, s.c.) (chronic/acute HT-AngII group) or NE (1.0 μg/g, twice per day, s.c.) (chronic/acute HT-NE group) to increase transiently systolic blood pressure (SBP); injections of AngII or NE were repeated for the whole period of observation. These doses of AngII and NE for injection were chosen based on published reports (Yang *et al*, 2003).

Systolic blood pressure was measured daily in conscious mice using tail-cuff plethysmography (Vistech System BP-2000, Apex, NC, USA) (Kurtz *et al*, 2005) as described previously (Wakisaka *et al*, 2008). Changes in SBP after injection of AngII, NE, or saline were measured on the first day of injection of these reagents.

Clinical signs of stroke were assessed by neurologic examinations at least three times per day by YW, including contralateral forelimb extension, circling behavior, or other motor dysfunction (Garcia *et al*, 1995). Mice were killed, and were perfused transcardially with 0.9% phosphate-buffered saline (PBS). Brains were excised and immersion-fixed in 10% formalin for determination of size and number of spontaneous ICH. Paraffin-embedded tissue was serially sectioned at 5 μm, resulting in approximately 2,000 to 2,400 sections of the entire brain of each mouse. The first and second sections of every set of five serial sections were stained with hematoxylin and eosin and with diaminobenzidine (DAB), respectively. Diaminobenzidine reacts with peroxidases in red blood cells, and facilitates precise identification of ICH, because DAB highlights hemorrhages and leaves nonhemorrhagic areas unstained (Wakisaka *et al*, 2008). All section stained with hematoxylin and eosin and DAB were screened, and images of ICH were captured and analyzed with ImageJ software (NIH, Bethesda, MD, USA) to quantify the size of hemorrhages. The size of ICH was estimated as follow: (area (mm²) of ICH on each section) $\times (25 \times 10^{-3}$ (mm): distance between successive DAB-stained sections).

Oxidative Stress and Matrix Metalloproteinases

Brain, heart, and blood samples were collected 12 ± 1 days after start of treatment. During this period, chronic/acute HT-AngII mice developed signs of stroke, and mice in other groups did not develop any neurologic signs. Blood samples were taken for measurement of serum creatinine using modified Fabinay and Ettingshausen method (Creatinine LiquiColor; Stanbio Lab, Boerne, TX, USA).

Brains were perfused transcardially with PBS, immediately removed, and cut sagittally in half. Analyses were conducted according to procedures described below.

Half of the fresh, unfixed brain of each mouse was frozen in TBS compound (Triangle Biomedical Sciences, Durham, NC, USA). Coronal sections (10 μm thick) were cut in a cryostat for the entire brain of each mouse. One of every five serial sections was stained with hematoxylin and eosin

and DAB for detection of ICH. We also examined vessels that appeared to be related to spontaneous ICH on serial sections of entire brains. Despite intensive investigation, and examination of more than 1,200 specimens/mouse in 10 mice, we detected only a small number of vessels that appeared to lead to spontaneous ICH and thus may be the 'culprit' vessels. The remaining sections were used for MMP *in situ* zymography and immunohistochemistry.

The middle one-third of fresh, unfixed other half of the brain (4 mm thick slice) was used to evaluate oxidative stress (superoxide), levels of MMPs by gelatin zymography, and gene expression. This slice of brain contains cerebral cortex, basal ganglia, thalamus, hippocampus, and upper part of brainstem (Paxinos and Franklin, 2000).

Evaluation of Oxidative Stress

Fresh unfixed brains were homogenized and sonicated in PBS containing protease inhibitors (protease inhibitor cocktail, Complete Mini; Roche Diagnostic, Mannheim, Germany) at 0°C to 5°C. Superoxide was quantified with lucigenin-enhanced chemiluminescence (Wakisaka *et al*, 2008). Fresh unfixed brains were homogenized and sonicated in PBS containing protease inhibitors (protease inhibitor cocktail, Complete Mini; Roche Diagnostic) at 0° to 5°C. Brain homogenates were placed in 0.5 mL PBS and 5 μmol/L lucigenin, and preincubated for 60 mins at room temperature with or without tiron (1 mmol/L), a superoxide dismutase (SOD) mimetic. Relative light units were measured for 10 mins. Background counts were determined and subtracted, and values were normalized per mg brain protein.

Nicotinamide adenine dinucleotide phosphate oxidase activity was estimated as levels of superoxide after adding NAD(P)H (1, 10, or 100 μmol/L) to brain homogenates with or without addition of tiron (1 mmol/L). Under all conditions, the tiron-inhibitable chemiluminescence value (relative light units/sec per mg brain protein) was used as a measure of superoxide. Total protein content was determined using a protein assay kit (Bio-Rad, Hercules, CA, USA).

Total SOD activity of brain homogenates was determined using the WST SOD assay kit (Sigma-Aldrich) as reported previously (Ukeda *et al*, 1999). The assay is based on competition of SOD and water-soluble tetrazolium salt (WST-1) for superoxide. One unit of SOD activity is defined as the amount of protein that results in 50% inhibition of WST-1 reduction. Superoxide dismutase activity is expressed as U/mg protein.

Quantitative Real-Time RT-PCR

RNA from the brain was prepared using the RNAeasy (Qiagen, Germantown, MD, USA) method following extraction with TRIZol reagent (Invitrogen, Carlsbad, CA, USA). Reverse transcription of RNA was performed using random hexamers as primers (Chu *et al*, 2002). Expression levels of pro-oxidant/NAD(P)H oxidase subunits (Nox1, Nox2, Nox4, and p47[phox]), antioxidants (SOD1, SOD2, SOD3, and catalase), nuclear factor-erythroid 2-related factor 2 (Nrf2),

and heme oxygenase-1 (HO-1) were determined by quantitative real-time RT-PCR using the TaqMan method (Chu *et al*, 2002). A housekeeping gene, *β*-actin (whose C_t was found to be consistent among all groups), was used as an internal control for each sample, using $\Delta\Delta C_t$ method. TaqMan primers and probes were purchased from Applied Biosystems (Foster City, CA, USA).

Gelatin Zymography

Brain samples were homogenized with lysis buffer (50 mmol/L Tris-HCl (pH 7.4), 150 mmol/L NaCl, 5 mmol/L CaCl$_2$, 0.05% Brij-35, and 1% Triton X-100). Matrix MMP-2 and -9 in homogenates were concentrated with gelatin-sepharose beads (Gelatin Sepharose 4B; GE Healthcare, Piscataway, NJ, USA) and analyzed by gelatin zymography. Briefly, brain homogenates were incubated overnight with Gelatin Sepharose 4B at 4°C. After incubation and centrifugation, samples were resuspended for 2 h in 200 μL of elution buffer containing dimethyl sulfoxide. Identical protein quantity from each sample was loaded onto 10% sodium dodecyl sulfate–polyacrylamide gels containing 0.1% gelatin as substrate (Bio-Rad). Standards included a mixture of human MMP-2 and -9 that express cleaved MMP-2, uncleaved MMP-2, and cleaved MMP-9 as molecular weights as 62, 68, and 92 kDa, respectively (Chemicon, Temecula, CA, USA), and murine MMP-9 (Chemicon) that express uncleaved MMP-9 as molecular weights as 105 and 98 kDa (Grossetete and Rosenberg, 2008). The organomercurial compound 4-aminophenyl-mercuric acetate (Sigma-Aldrich) was used to activate murine MMP-9 standard. After electrophoresis, the gel was washed in renaturation buffer containing 2.7% Triton X-100 to remove the sodium dodecyl sulfate. Gels were incubated for 96 h at 37°C with a developing buffer (50 mmol/L Tris, 40 mmol/L HCl, 5 mmol/L CaCl$_2$, 200 mmol/L NaCl, and 0.2% Brij-35; Invitrogen). After incubation, gels were stained with 0.25% Coomassie blue R-250 (Bio-Rad) for 30 mins in 10% acetic acid and 30% methanol. Gels were destained with a solution containing 10% acetic acid and 30% methanol until clear bands of gelatinolysis appeared on a dark blue background. The gels were scanned for densitometry. Relative gelatinolytic activity against human MMP-2 standard or murine MMP-9 standard, as appropriate, was quantified by measurement of optical density using the ImageJ software (NIH).

In Situ Zymography and Immunofluorescence

In situ gelatinolytic activity was assessed on frozen brain sections 10 μm in thickness using a commercially available kit (EnzCheck Gelatinase Assay Kit; Invitrogen). Sections were incubated with DQ gelatin conjugate, a fluorogenic substrate, at 37°C for 1 h. Then brain sections were washed and fixed in 4% paraformaldehyde in PBS. Cleavage of DQ gelatin by MMPs resulted in a green fluorescent product (wavelengths: excitation, 495 nm; emission, 515 nm). Sections incubated without DQ gelatin were not fluorescent. Some brain sections were also labeled with several primary antibodies against astrocytes (GFAP; polyclonal, chicken,

1:1,000; Chemicon), endothelial cells (von Willebrand factor (vWF); polyclonal, rabbit, 1:500; Chemicon) or CD31 (monoclonal, rat, 1:100; Abcam, Cambridge, MA, USA), collagen type IV (polyclonal, rabbit, 1:100; Chemicon; or polyclonal, goat, 1:200; Chemicon), MMP-9 (polyclonal, rabbit, 1:100; Chemicon), and 8-hydroxyguanosine (polyclonal, goat, 1:200; GeneTex, San Antonio, TX, USA). Neurons were also stained with a mouse antineuron-specific nuclear protein (NeuN, 1:100; Chemicon) using the MOM kit (Vector Laboratories, Burlingame, CA, USA). Sections were incubated overnight at 4°C, rinsed with PBS, and incubated for 1 h at room temperature with secondary antibodies labeled with Alexa Fluor 568 dye or Alexa Fluor 647 dye (Invitrogen). Sections were examined with Bio-Rad MRC-1024 laser scanning confocal microscope. Sections incubated in the absence of the primary antibodies were not fluorescent.

Statistics

Results are expressed as mean ± s.e. Analysis of variance followed by Bonferroni test was used for comparison of multiple groups. Mann–Whitney U-test was used for comparison of two groups. A probability value of $P < 0.05$ was considered significant. Cumulative incidence of signs of stroke was evaluated using a Kaplan–Meier test and the difference among groups was analyzed by log-rank test.

Results

Spontaneous Intracerebral Hemorrhage in Hypertensive Mice

Systolic blood pressure: Systolic blood pressure increased from 103 ± 3 (mean ± s.e.) to 164 ± 2 mm Hg 7 days after the initiation of chronic hypertension (Figure 1A). Systolic blood pressure increased for about 20 to 40 mins after injections of NE or AngII, and was greater in chronic/acute HT-NE mice than in chronic/acute HT-AngII mice. In addition, SBP in chronic/acute HT-AngII mice returned to basal values earlier (∼20 mins) than in chronic/acute HT-NE mice (∼40 mins) (Supplementary Figure I). Acute hypertension after injections of NE or AngII did not affect basal levels of SBP in chronically hypertensive mice (Figure 1A).

Compared with control mice, all four groups of hypertensive mice developed cardiac hypertrophy. Serum creatinine tended to increase (not significant, NS) in chronically hypertensive mice and in chronic/acute HT-NE mice without ICH, and increased significantly in chronic/acute HT-AngII mice without and with ICH (Supplementary Table I).

Signs of stroke: Only 1 of 15 chronically hypertensive mice, without acute hypertension, showed signs of stroke. Eleven of 15 chronic/acute HT-AngII mice (73%) and 6 of 15 chronic/acute HT-NE mice (40%) developed signs of stroke 15 ± 1 and 20 ± 3

days after start of AngII infusion and L-NAME, respectively ($P < 0.05$; Figure 1B).

Histologic analysis: All mice with signs of stroke in the chronic/acute HT-NE group and chronic/acute HT-AngII group developed multiple ICHs that were distributed widely in the brain (Figures 1C–1G). There were more ICH in cerebral cortex, basal ganglia, thalamus, and brainstem in chronic/acute HT-AngII mice than chronic/acute HT-NE mice (Figure 1F). Volume of ICH in basal ganglia and thalamus of chronic/acute HT-AngII mice was larger than that of chronic/acute HT-NE mice (Figure 1G).

In one chronically hypertensive mouse that developed neurologic signs, there were a few ICH in brainstem. Mice without neurologic signs in all groups did not have histologically detectable ICH. In a preliminary study, 1 of 10 mice treated with AngII infusion and AngII injection, without L-NAME, developed one ICH in cerebral cortex, without developing signs of stroke. No mouse treated with AngII infusion and NE injection, without L-NAME, developed neurologic signs or a histologically detectable ICH (data not shown).

Despite intensive histologic analysis, only a few ischemic lesions were found in these mice. Ischemic lesions were separate from spontaneous ICH. No ICH lesion was found in an ischemic region.

Oxidative Stress and Matrix Metalloproteinases in Spontaneous Intracerebral Hemorrhage

Oxidative stress: The level of superoxide in the brain was low in control mice, increased significantly in chronically hypertensive mice, increased further in chronic/acute HT-AngII mice without ICH, and was highest in chronic/acute HT-AngII mice with ICH (Figure 2A). In contrast, the level of superoxide did not increase further in chronic/acute HT-NE mice compared with chronically hypertensive mice, even though the transient increase in SBP after injections of NE was greater and more sustained than after injections of AngII (Supplementary Figure I). Nicotinamide adenine dinucleotide phosphate oxidase activity increased in parallel with changes in superoxide (Figure 2B).

Expression of Nox1 and Nox4 increased significantly in most groups with chronic and acute hypertension (Figure 3A). There were no differences in expression of Nox2 and p47^{phox} among groups (Figure 3A).

Expression of SOD1, SOD2, SOD3, and catalase decreased significantly in most groups with chronic and acute hypertension (Figure 3B). Total SOD activity also decreased in most groups of hypertensive mice (Figure 3C). Expression of Nrf2, a redox-sensitive transcription factor that upregulates antioxidant genes, was decreased significantly, and expression of HO-1, a stress enzyme induced by several stimuli including oxidative stress, was
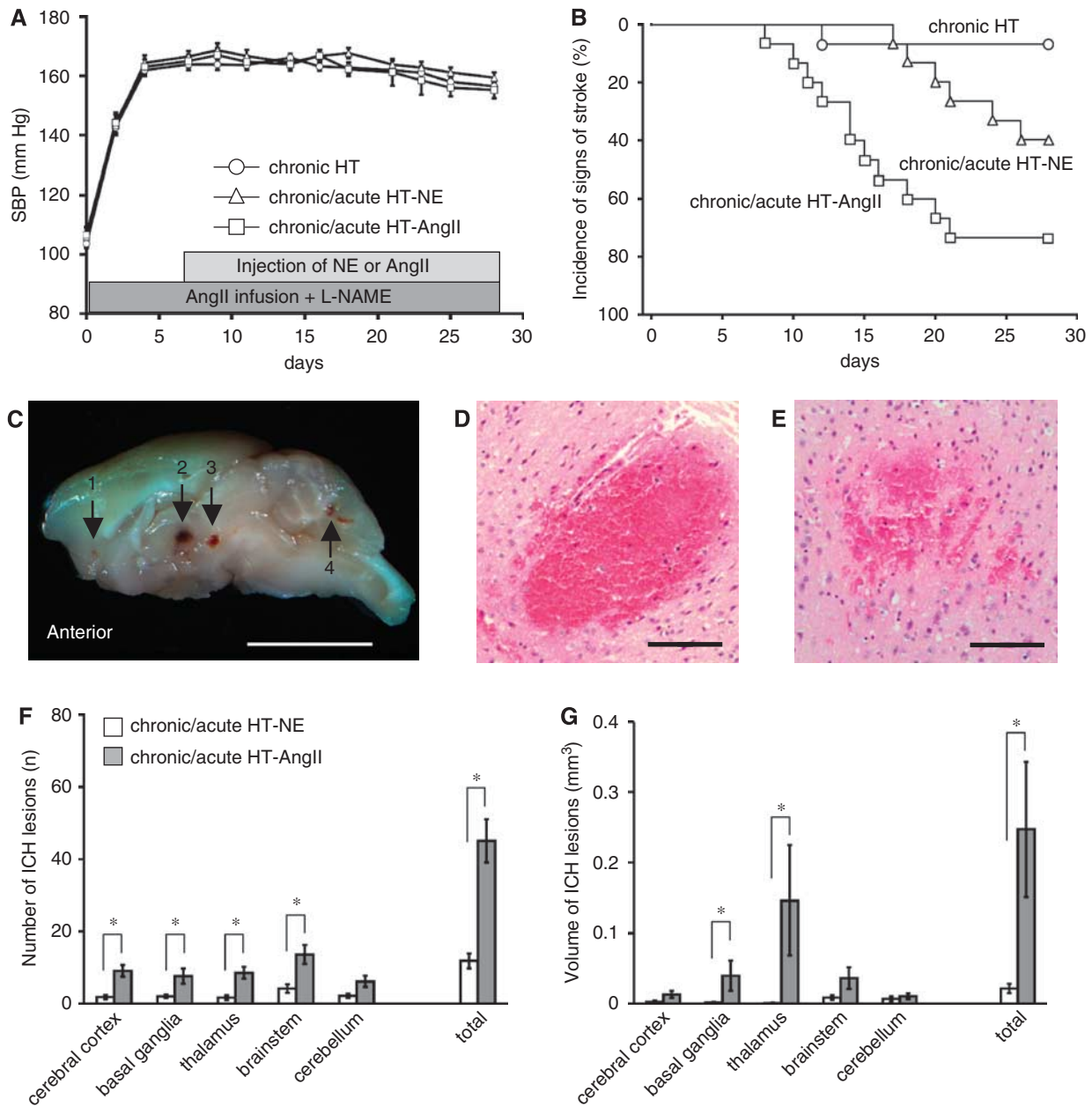
Figure 1 (A) Systolic blood pressure (SBP). HT, hypertension; NE, norepinephrine; AngII, Angiotensin II; L-NAME, N^{ω}-nitro-L-arginine methyl ester. Values are mean ± s.e. $n = 15$ in each group. (B) Kaplan–Meier plot of signs of stroke. $n = 15$ in each group. (C) Sagittal section through brain of chronic/acute HT-AngII mouse. Arrows indicate spontaneous ICH in (1) cerebral cortex, (2) thalamus, (3) upper brainstem, and (4) cerebellum. Bar: 5 mm. (D and E) Hematoxylin and eosin staining of brain sections with spontaneous ICH in thalamus of chronic/acute HT-AngII mouse. (D) Confluent ICH. (E) Patchy ICH. Bar: 200 μm. (F) Number and (G) volume of spontaneous ICH per mouse. $n = 6$ in chronic/acute HT-NE mice and $n = 11$ in chronic/acute HT-AngII mice. *$P < 0.05$.

increased significantly in chronic/acute HT-AngII mice without and with ICH (Figure 3D).

Matrix metalloproteinases: Levels of MMP-9 and -2 in brain homogenates were evaluated using gelatin zymography. Gelatinolytic activity of MMP-9 was barely detectable in control mice (Figures 4A and 4B). Levels of MMP-9 (98 kDa) tended to increase (NS) in chronically hypertensive mice and in chronic/acute HT-NE mice without ICH, increased significantly in chronic/acute HT-AngII mice without ICH, and increased further in chronic/acute HT-AngII mice with ICH. In contrast to MMP-9, bands corresponding to the latent form of MMP-2 were visible in control mice but did not change significantly among groups. No detectable levels of the cleaved form of MMP-9 and -2 were seen in any group.
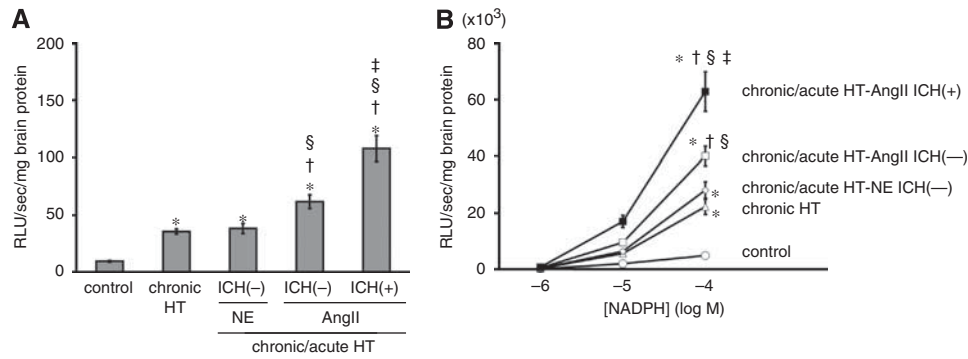
Figure 2 (**A**) Basal level of superoxide and (**B**) NAD(P)H oxidase activity in brain homogenates. $n = 10$ in each group. $*P < 0.05$ versus control mice; $†P < 0.05$ versus chronically hypertensive (chronic HT) mice; $§P < 0.05$ versus chronic/acute HT-NE mice without ICH; $‡P < 0.05$ versus chronic/acute HT-AngII mice without ICH.
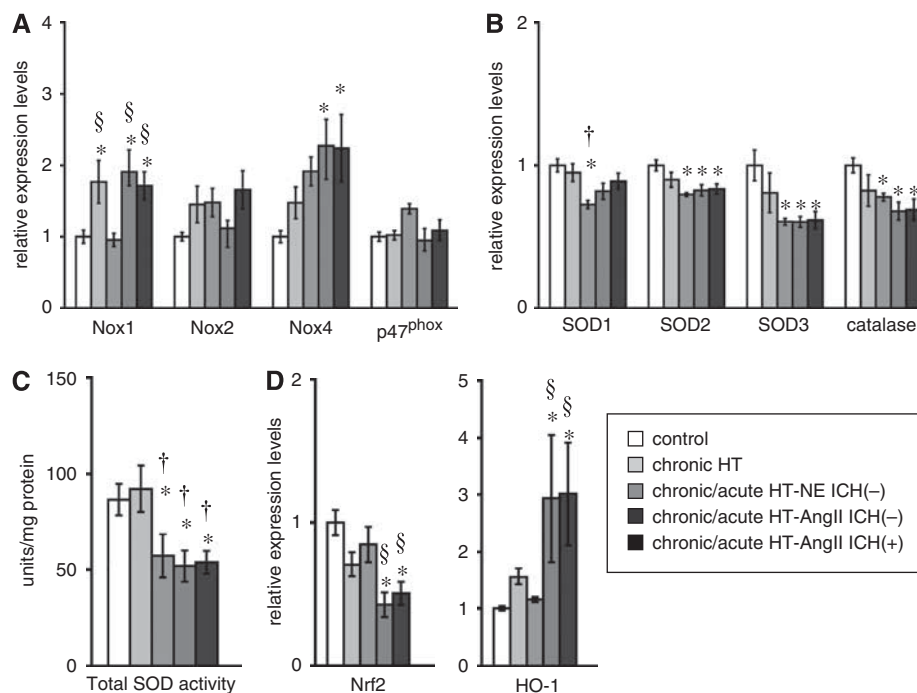

Figure 3 Relative expression of mRNA of (**A**) NAD(P)H oxidase subunits, (**B**) antioxidants (SOD1, SOD2, SOD3, and catalase), and (**D**) Nrf2 and HO-1 in brain. (**C**) Total activity of SODs in brain. $n = 10$ in each group. $*P < 0.05$ versus control mice; $†P < 0.05$ versus chronically hypertensive (chronic HT) mice; $§P < 0.05$ versus chronic/acute HT-NE mice without ICH.

In situ zymography did not show detectable levels of in situ gelatinolytic activity in the brain of control mice (Figure 4C). Although the cleaved form of MMP-9 or -2 was not detected by gelatin zymography, in situ zymography revealed a low level of gelatinolytic activity in chronically hypertensive mice and in chronic/acute HT-NE mice without ICH. In situ gelatinolytic activity was clearly present in the brain of chronic/acute HT-AngII mice without and with ICH.

Immunohistochemistry combined with in situ zymography suggested that in situ gelatinolytic activity was colocalized mainly on nucleus of neurons and rarely on astrocytes (Figure 4D). No
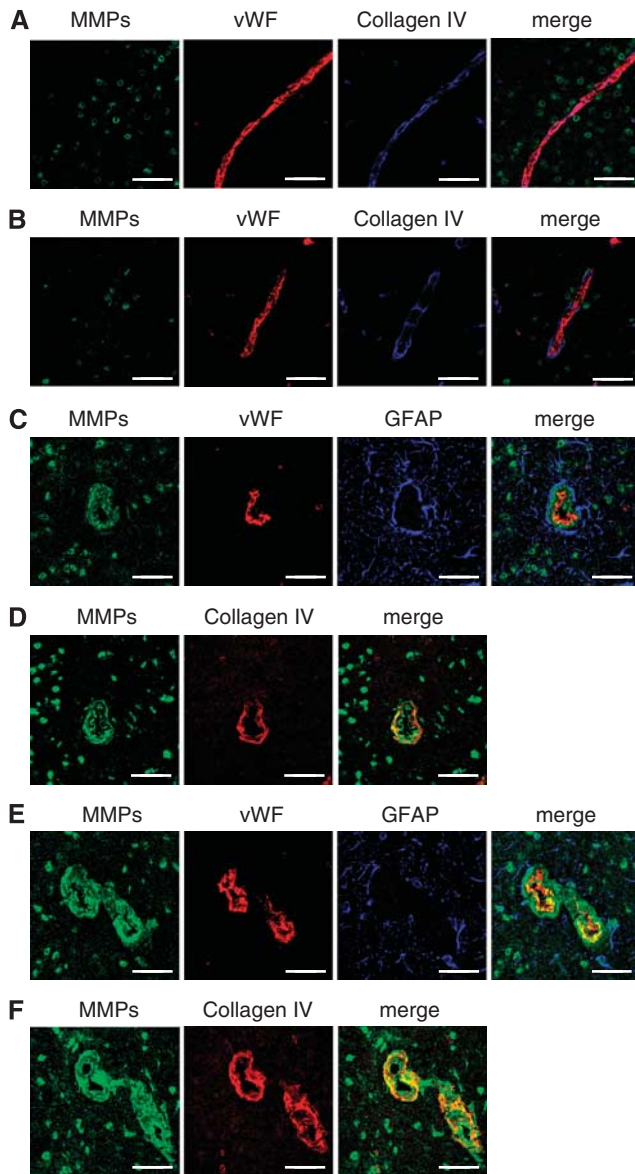
in situ gelatinolytic activity was found on cerebral vessels of chronically hypertensive mice (Figure 5A) or chronic/acute HT-NE mice without ICH (Figure 5B); in situ gelatinolytic activity was occasionally found on cerebral vessels of chronic/acute HT-AngII mice without (Figures 5C and 5D) and with ICH (Figures 5E and 5F). On these vessels, in situ gelatinolytic activity was detected diffusely in endothelial cells and in the ECM (Figures 5C–5F).

Colocalization of in situ gelatinolytic activity and 8-hydroxyguanosine, a marker of oxidative stress, was observed in neurons, endothelial cells, and ECM (Figure 6). Most in situ gelatinolytic activity on neurons, endothelial cells, and ECM colocalized
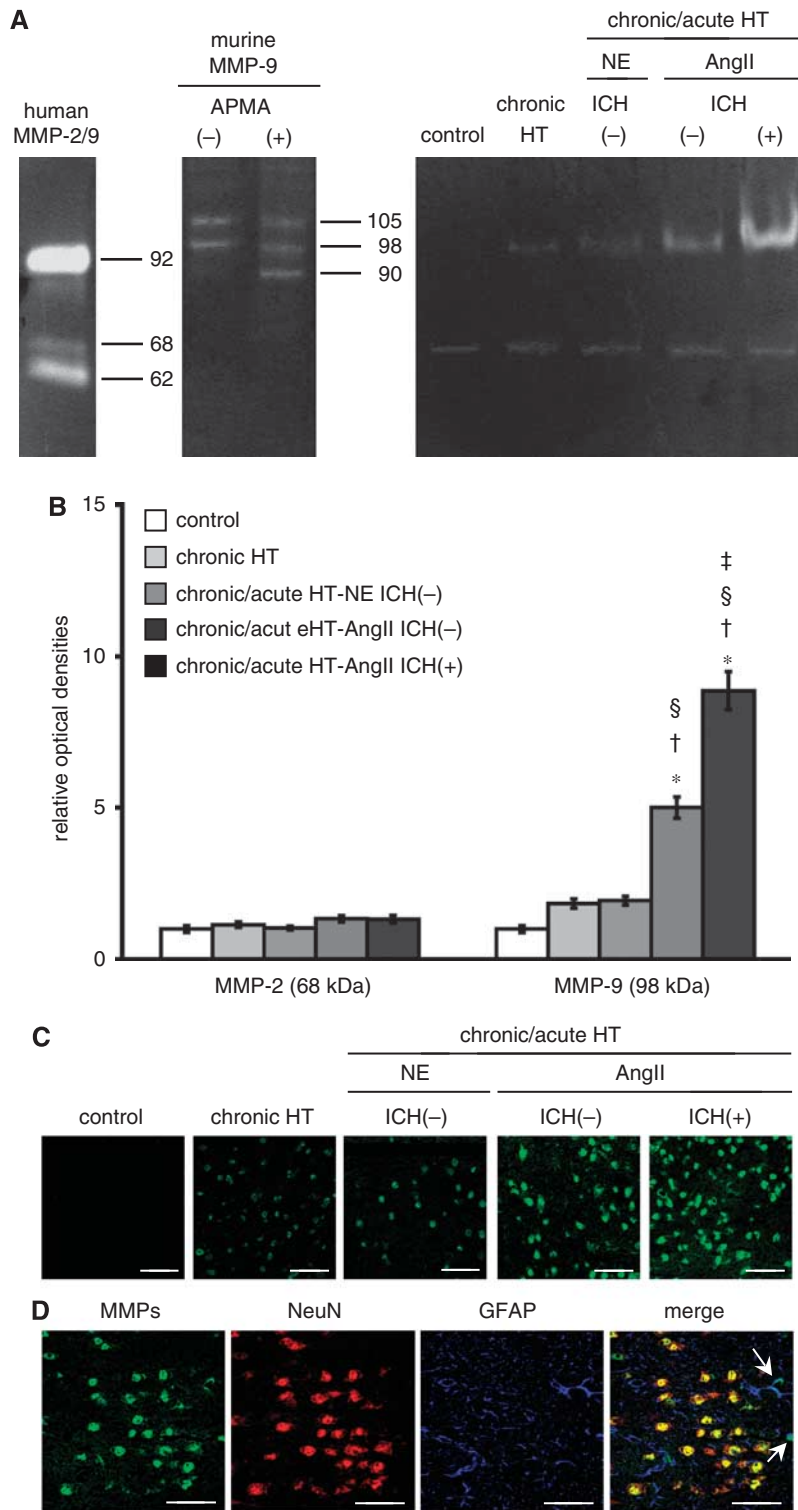
Figure 4 (**A**) Gelatin zymography showing gelatinolytic activity of MMP-2 (68 kDa, latent form; 62 kDa, cleaved form) and MMP-9 (98 and 105 kDa, latent form; 90 kDa, cleaved form). APMA, chemical activator for MMP-9. $n = 10$ in each group. (**B**) Relative optical density of MMP-2 (68 kDa) and MMP-9 (98 kDa). $n = 10$ in each group. *$P < 0.05$ versus control mice. †$P < 0.05$ versus chronically hypertensive (chronic HT) mice. §$P < 0.05$ versus chronic/acute HT-NE mice without ICH; ‡$P < 0.05$ versus chronic/acute HT-AngII mice without ICH. (**C** and **D**) In situ zymography of brain sections from thalamus. (**C**) Brain sections of each group. (**D**) Brain sections of chronic/acute HT-AngII mouse without ICH showing in situ gelatinolytic activity on neurons (NeuN) and on astrocytes (GFAP) (arrows). Bars: 50 μm.

Figure 5 *In situ* gelatinolytic activity on cerebral microvessels in thalamus of (**A**) chronically hypertensive mouse, (**B**) chronic/acute HT-NE mouse without ICH, (**C** and **D**) chronic/acute HT-AngII mouse without ICH, and (**E** and **F**) chronic/acute HT-AngII mouse with ICH. Panels **E** and **F** were obtained at a distant site from the ICH. Panels **C** and **D**, and **E** and **F** were derived from adjacent sections, respectively. NeuN, neurons; GFAP, astrocytes; vWF, endothelial cells; collagen IV, extracellular matrix. Bars: 50 μm.

immunohistochemically with MMP-9 (Supplementary Figure II).

Vessels that appeared to lead toward regions with ICH (Figures 7A and 7B) showed prominent *in situ* gelatinolytic activity on ECM and on endothelial cells, compared with vessels that were outside ICH lesion, even though the vessels seemed to branch from the same vessel (Figures 7C–7E). In addition, astrocytic endfeet surrounding vessels that ran into ICH lesion expressed *in situ* gelatinolytic activity

(Figure 7C). Colocalization of *in situ* gelatinolytic activity and oxidative stress on ECM and endothelial cells was prominent in vessels that appeared to be associated with ICH (Figures 7D and 7E). Similar findings were seen in five other small cerebral vessels leading toward regions with ICH, based on examination of more than 1,200 serial sections/mouse in 10 chronic/acute HT-AngII mice with ICH. We cannot exclude the possibility, however, that oxidative stress and increased MMP levels are secondary to, rather than preceding, ICH.

Discussion

There are several major findings in this study. First, we have developed a new model of spontaneous ICH in mice. The experimental model is relatively easy, very consistent, and may be used in genetically altered mice. Mice with acute hypertension, induced either by AngII or NE injection, superimposed on chronic hypertension, developed spontaneous ICH. This finding suggests that acute hypertension may contribute to spontaneous ICH during chronic hypertension. Second, incidence, number, and size of ICH were greater in mice that received injections of AngII than NE, even though injections of NE produced larger and longer increases in SBP than injections of AngII. Oxidative stress was greater in chronic/acute HT-AngII mice than chronic/acute HT-NE mice, which suggests that increases in AngII-mediated oxidative stress contribute to spontaneous ICH in our model. The increase in AngII-mediated oxidative stress was associated with concomitant upregulation of Nox1 and Nox4, and downregulation of antioxidant enzymes. Third, increases in MMP-9 paralleled levels of superoxide and NAD(P)H oxidase activity. In addition, increased levels of MMP-9 were noted on endothelial cells and ECM of cerebral vessels that appeared to be associated with spontaneous ICH. These findings are compatible with the hypothesis that AngII-mediated oxidative stress leads to increased levels of MMP-9, alteration of matrix of cerebral blood vessels, and development of spontaneous ICH during acute, superimposed on chronic, hypertension.

Experimental Model of Spontaneous Intracerebral Hemorrhage

There has been substantial progress in understanding the role of oxidative stress and MMPs in hemorrhagic transformation after ischemic stroke and brain injury after ICH (Gasche *et al*, 2001; Yang *et al*, 2007; Zhao *et al*, 2007; Grossetete and Rosenberg, 2008). In contrast, there has been limited progress in understanding the pathophysiology of spontaneous ICH, in part because there is no experimental model of spontaneous ICH that mimics
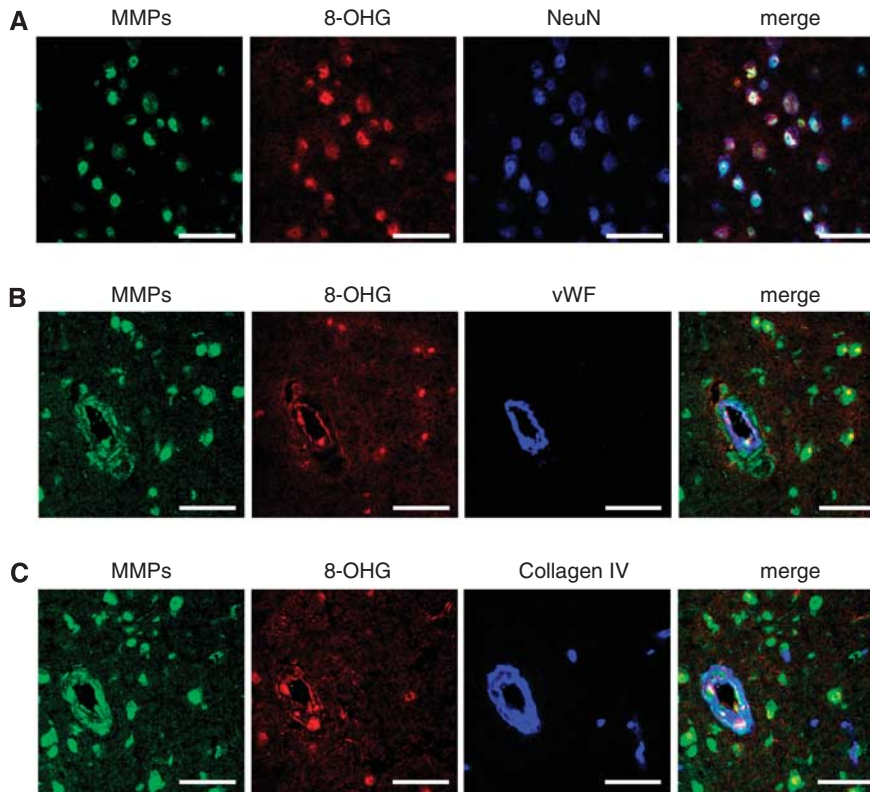
Figure 6 *In situ* gelatinolytic activity and oxidative stress on (**A**) neurons, (**B**) endothelial cells, and (**C**) extracellular matrix of vessels in thalamus of chronic/acute HT-AngII mouse without ICH. 8-OHG: 8-hydroxyguanosine, an oxidative stress marker. Images of (**B**) and (**C**) were derived from adjacent sections. Findings in thalamus are provided because volume of ICH was greater in thalamus than other regions. Findings were similar in other regions. Bars: 50 μm.

ICH in hypertensive humans (NINDS ICH Workshop Participants, 2005).

Stroke-prone spontaneous hypertensive rats are useful for studying stroke. Stroke-prone spontaneous hypertensive rats, however, generally develop ischemic stroke and, when hemorrhage occurs, ICH usually is secondary to hemorrhagic transformation of an ischemic stroke (Sadoshima *et al*, 1981). A model to examine consequences of ICH in experimental animals is to inject autologous blood or collagenase into brain (MacLellan *et al*, 2008). These approaches, however, are not very useful for investigation of mechanisms that lead to spontaneous ICH. Therefore, it is necessary to develop alternative animal models to investigate fundamental mechanisms of spontaneous ICH (NINDS ICH Workshop Participants, 2005).

We developed the first model of spontaneous ICH in chronically hypertensive R+/A+ mice (Iida *et al*, 2005; Wakisaka *et al*, 2008). A limitation of this model is that, because the mice are double transgenic, it is difficult to cross them with other genetically altered mice. Therefore, we developed a second model of spontaneous ICH in wild-type mice that facilitates studies in genetically altered mice. We found that mice with AngII-induced acute hypertension, superimposed on chronic hypertension, have a high incidence of spontaneous ICH. In this model,

the location of ICHs was similar to the distribution in hypertensive humans: basal ganglia, thalamus, brainstem, cerebellum, as well as cerebral cortex (Xi *et al*, 2006). Thus, mice with acute, superimposed on chronic, hypertension appear to be a useful model to study mechanisms that lead to ICH associated with hypertension.

Acute Hypertension and Intracerebral Hemorrhage

Although chronic hypertension is a major risk factor for spontaneous ICH in humans, spontaneous ICH was rare in chronically hypertensive mice in this study, perhaps because of the short duration of the study. Chronically hypertensive R+/A+ mice, however, with mean SBP of about 150 to 160 mm Hg, also fail to develop neurologic signs, even in a much longer study (Baumbach *et al*, 2003). Therefore, chronic hypertension with moderate increases of blood pressure does not seem to be sufficient to produce spontaneous ICH, at least in these mouse models. In contrast, mice with AngII-induced acute hypertension, superimposed on chronic hypertension, frequently and rapidly developed spontaneous ICH.

Acute increases in blood pressure or cerebral blood flow may contribute to rupture of perforating
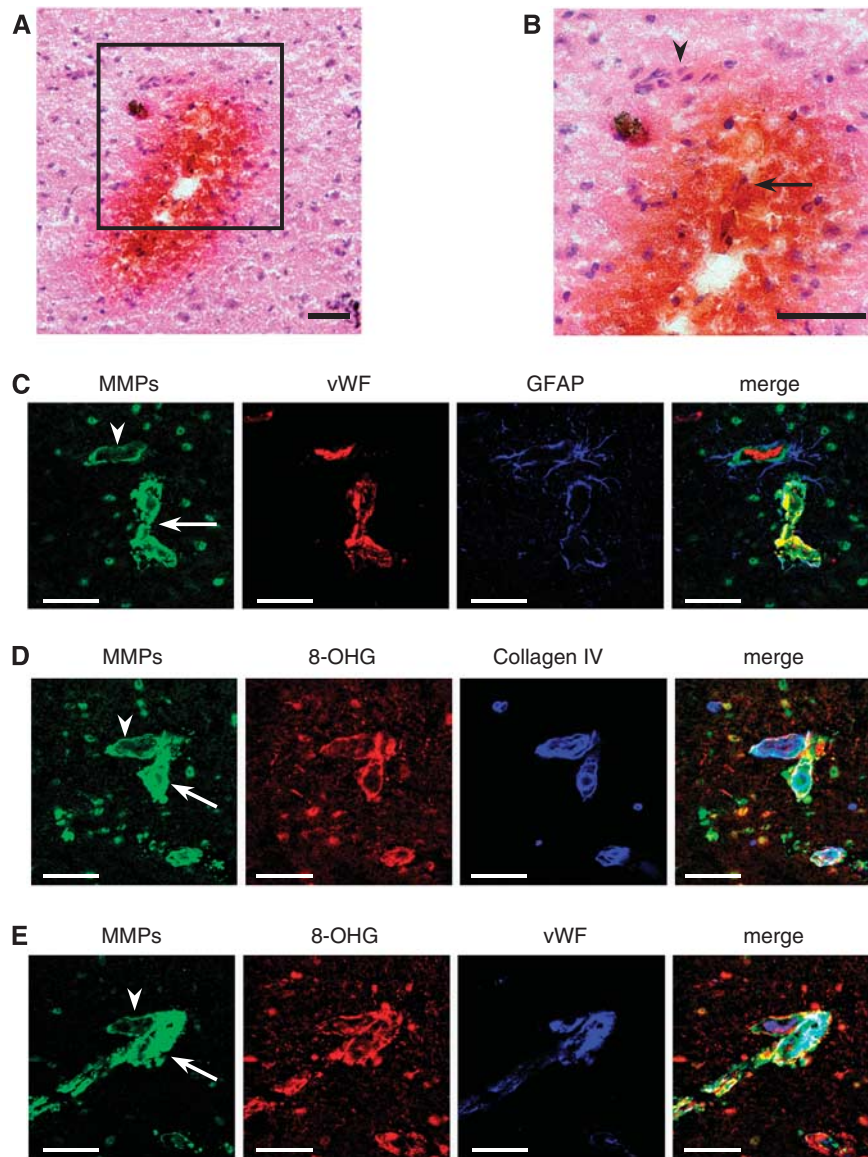
Figure 7 Vessel that appeared to lead toward a region with spontaneous ICH in thalamus of chronic/acute HT-AngII mouse with ICH. (**A** and **B**) hematoxylin and eosin staining combined with diaminobenzidine staining. Image in box of **A** is magnified in **B**. Arrow indicates vessel running into the ICH lesion. Arrowhead indicates vessel running outside ICH lesion. (**C**–**E**) *In situ* gelatinolytic activity on vessels. Images of **B**–**E** were derived from serial sections. Bars: 50 μm.

cerebral vessels (Caplan, 1994). Large morning surges in blood pressure are a risk factor for ICH (Metoki *et al*, 2006). Increased activity of the renin–angiotensin system may contribute to acute hypertension (Vaughan and Delanty, 2000). Therefore, it seems reasonable to suggest that AngII-induced acute hypertension is an important risk factor for ICH, especially when superimposed on chronic hypertension.

Oxidative Stress and Intracerebral Hemorrhage

In our first model of spontaneous ICH in R+/A+ mice, superoxide and NAD(P)H oxidase activity increased before ICH, and increased further when R+/A+ mice developed spontaneous ICH (Wakisaka *et al*, 2008). Hypertension produced by the renin–angiotensin system is associated with increases in superoxide in blood vessels (Didion *et al*, 2002). These increases in oxidative stress induce dysfunction and perhaps cell death of endothelium and vascular muscle (Didion and Faraci, 2003; Burlacu *et al*, 2001). Thus, in the model of ICH in R+/A+ mice, we speculated that enhanced superoxide through activation of NAD(P)H oxidase has an important role in the pathogenesis of hypertensive ICH. We did not determine, however, which subunits of NAD(P)H oxidase are associated with spontaneous ICH (Wakisaka *et al*, 2008).

In this study, we confirmed that chronic hypertension increases superoxide and NAD(P)H oxidase activity in the brain, and also found that expression of Nox1 was increased in the brain of chronically hypertensive mice. We also found that superoxide and NAD(P)H oxidase activity increased further in the brain when chronic hypertension was combined with AngII-induced acute hypertension, even before developing spontaneous ICH. Expression of Nox1 and Nox4 was increased, and expression of SOD2 and SOD3 and total SOD activity was decreased in the brain, when AngII-induced acute hypertension was produced during chronic hypertension. Acute hypertension produced by transverse aortic coarctation also increases superoxide and NAD(P)H oxidase activity in brain (Poulet *et al*, 2006). The finding is compatible with our observation that AngII-induced acute hypertension increased oxidative stress in the brain during chronic hypertension.

Our finding that expression of Nox1 and Nox4 is increased in brains of chronic/acute HT-AngII mice is concordant with previous reports that Nox1 and Nox4, in addition to Nox2, are expressed in normal mouse brain (Infanger *et al*, 2006). Furthermore, the findings are compatible with previous reports that Nox1 and Nox4 have a pivotal function in increasing superoxide levels in vessels and in brain of mouse during increases in activity of renin–angiotensin system (Matsuno *et al*, 2005; Inaba *et al*, 2009).

Conversely, the finding of decreased expression of SOD2 and SOD3 and total SOD activity in brains of chronic/acute HT-AngII mice is different from other studies, which observed that hypertension-related oxidative stress usually stimulates antioxidant mechanisms including SODs in vessels (Fukai *et al*, 1999). We also found that expression of Nrf2 was decreased in chronic/acute HT-AngII mice without and with ICH. Nrf2 is a critical transcription factor that upregulates several antioxidants including SODs (Dong *et al*, 2008). AngII, however, may inhibit nuclear translocation of Nrf2, resulting in downregulation of target genes (Alba *et al*, 2008). Thus, we speculate that decreased levels of SODs in our study could be explained, in part, by impairment of mechanisms that upregulate SOD expression through Nrf2.

When chronically hypertensive mice received injections of NE, SBP increased more than chronic/acute HT-AngII mice, but incidence of ICH was less in chronic/acute HT-NE mice. In contrast to chronic/acute HT-AngII mice, chronic/acute HT-NE mice did not show further increases in oxidative stress compared with chronically hypertensive mice. These results are in accordance with previous studies showing that AngII-induced, but not NE-induced, hypertension was associated with an increase in level of superoxide through NAD(P)H oxidase activity (Laursen *et al*, 1997). We found that expression of Nox4 was upregulated and levels of SOD and catalase were downregulated in chronic/acute HT-NE mice. In contrast, expression of Nox1 was similar to that of control mice when acute hypertension was produced with injections of NE in chronically hypertensive mice.

Mechanisms responsible for differential regulation of Nox1 and Nox4 in chronic/acute HT-NE mice are not clear in this study. We also found, however, that expression of HO-1 remained low in chronically hypertensive mice and chronic/acute HT-NE mice, and was upregulated in chronic/acute HT-AngII, even before developing spontaneous ICH. HO-1 is a stress enzyme that is induced by oxidative stress, including superoxide and hydrogen peroxide (Immenschuh and Ramadori, 2000). Thus, low levels of HO-1 in chronically hypertensive mice and in chronic/acute HT-NE mice may support the finding that levels of oxidative stress in chronic/acute HT-NE mice remained comparable to those of chronically hypertensive mice. Increased expression of HO-1 also may reflect enhanced oxidative stress in chronic/acute HT-AngII mice. Therefore, greater incidence of spontaneous ICH during AngII- than NE-induced acute hypertension may be related to the greater prooxidant effects of AngII than NE.

Collectively, the findings suggest that increases in oxidative stress, in part through concomitant upregulation of Nox1 and Nox4 and downregulation of antioxidant enzymes, may contribute to spontaneous ICH in chronic/acute HT-AngII mice.

Matrix Metalloproteinases and Intracerebral Hemorrhage

Matrix metalloproteinases are involved in degradation of basal lamina and ECM (Woessner, 1991). These are reported to disrupt the blood–brain barrier and to contribute to hemorrhagic transformation after focal cerebral ischemia (Gasche *et al*, 2001; Yang *et al*, 2007; Zhao *et al*, 2007). They also induce brain injury after ICH (Grossetete and Rosenberg, 2008). Expression and activity of MMPs in spontaneous ICH, however, have not been elucidated.

In this study, control mice did not show gelatinolytic activity of MMP-9 by gelatin zymography, which is consistent with the concept that MMP-9 is not constitutively expressed in mammalian brain (Rosenberg *et al*, 1996). In chronically hypertensive mice and chronic/acute HT-NE mice, MMP-9 (98 kDa) was detectable by gelatin zymography, but was not significantly greater than in control mice. In mice with chronic/acute HT-AngII mice without ICH, however, gelatinolytic activity of MMP-9 (98 kDa) was increased, and increased further when chronic/acute HT-AngII mice developed spontaneous ICH, in parallel with the changes in oxidative stress. In contrast to MMP-9, MMP-2 did not differ in the various groups, which is consistent with the concept that astrocytes constitutively produce MMP-2 in an inactive form, and that MMP-2 does not change after experimental focal ischemia (Gasche *et al*, 2001; Liu and Rosenberg, 2005).

Matrix metalloproteinase 9 with molecular weight of 98 or 105 kDa has been proposed to be 'pro-MMP-9' (Grossetete and Rosenberg, 2008). Matrix metalloproteinases are secreted as latent 'pro-MMPs' by all types of brain cells, including neurons, astrocytes, and endothelial cells (Cunningham *et al*, 2005). Pro-MMPs are maintained in a catalytically inactive state by the interaction between the cysteine residue in the prodomain and the zinc ion at the catalytic site (cysteine switch) (van Wart and Birkedal-Hansen, 1990). In several studies *in vitro*, pro-MMPs were fully activated by disruption of the cysteine switch, followed by removal of the propeptide domain, with a corresponding loss of about 10 kDa in molecular mass (van Wart and Birkedal-Hansen, 1990). Many studies *in vivo*, however, showed that the predominant forms of MMP-9 detected in gelatin zymography were an uncleaved form of MMP-9 with molecular weight 105 or 98 kDa (Gasche *et al*, 2001; Grossetete and Rosenberg, 2008), and these uncleaved forms of MMP-9 may be functionally activated (Gasche *et al*, 2001).

Because gelatin zymography does not accurately represent the actual proteolytic activity in the brain (Gasche *et al*, 2001; Cunningham *et al*, 2005), and to determine whether MMP-9 was enzymatically active in brain tissue in our study, we performed *in situ* zymography on brain sections. First, no active MMPs were detectable in control mice, and levels of active MMPs were low in chronically hypertensive mice and chronic/acute HT-NE mice. Second, active MMPs were clearly identified in the brain of chronic/acute HT-AngII mice without and with ICH, mainly on neurons with a distinct nuclear localization. Third, although most cerebral vessels did not present active MMPs in these mice, active MMPs were occasionally found on endothelial cells and ECM of cerebral vessels in chronic/acute HT-AngII mice without ICH. Intensity of active MMPs on cerebral vessels was highest on those vessels that appeared to be associated with ICH. Interestingly, in contrast to nuclear localization of active MMPs in neurons, active MMPs appeared to localize diffusely on endothelial cells and ECM of cerebral vessels. Immunohistochemistry against MMP-9 indicated that active MMPs that were observed with *in situ* zymography were mainly MMP-9. Therefore, our results indicated that enzymatically active MMP-9 was increased on neurons and on cerebral vessels of chronic/acute HT-AngII mice, even before developing spontaneous ICH, and also suggested that active MMP-9 expressed on cerebral vessels may contribute to the ICH.

Active MMPs colocalized with 8-hydroxyguanosine, an oxidative stress marker, as shown by *in situ* zymography. In addition, levels of MMP-9 by gelatin zymography paralleled levels of superoxide and NAD(P)H oxidase activity. These findings support the concept that induction and activation of MMPs are upregulated by oxidative stress, including superoxide (Gasche *et al*, 2001; Liu and Rosenberg, 2005; Rajagopalan *et al*, 1996). Thus, we suggest that AngII-induced acute, superimposed on chronic, hypertension increased levels of oxidative stress and activity of MMP-9 in brain tissue, leading to degradation of endothelial cells and ECM of cerebral vessels, predisposing to spontaneous ICH.

Limitations of Study

There are several limitations in the present study. First, although we found expression of 8-hydroxyguanosine (especially on blood vessels and neurons of chronic/acute HT-AngII mice), we cannot rule out other sources of oxidative stress, such as other brain cells and infiltrating inflammatory cells. Second, although active MMP-9 was observed on neurons and cerebral vessels, the cellular sources of MMP-9 are not clear. A contribution of inflammatory cells may also be important, because reactive microglia and neutrophils may be a key cellular source of MMP-9 (Zhao *et al*, 2007). Third, we did not elucidate the role of L-NAME in ICH. We speculate, however, that L-NAME may contribute to ICH by increasing MMP-9 activity (Shin *et al*, 2007).

Conclusion

Susceptibility to ICH was greater when acute hypertension was produced by AngII than by NE, probably because of the prooxidant effects of AngII. Thus, we speculate that acute hypertension induced by AngII, and less by NE, may be critical in spontaneous ICH during chronic hypertension through oxidative stress and MMP-9. The findings extend previous studies that suggest that a large morning surge in blood pressure is a risk factor for ICH, probably through activation of the renin–angiotensin system and the sympathetic nerve system (Metoki *et al*, 2006; Vaughan and Delanty, 2000). Thus, in addition to treatment of hypertension, inhibition of the renin–angiotensin system may be a critical target to prevent spontaneous ICH in hypertensive patients.

Acknowledgements

Disclosure/conflict of interest

The authors declare no conflict of interest.

References

Alba G, El Bekay R, Chacón P, Reyes ME, Ramos E, Oliván J, Jiménez J, López JM, Martín-Nieto J, Pintado E, Sobrino F (2008) Heme oxygenase-1 expression is

68

down-regulated by angiotensin II and under hypertension in human neutrophils. *J Leukoc Biol* 84:397–405

Baumbach GL, Sigmund CD, Faraci FM (2003) Cerebral arteriolar structure in mice overexpressing human renin and angiotensinogen. *Hypertension* 41:50–5

Burlacu A, Jinga V, Gafencu AV, Simionescu M (2001) Severity of oxidative stress generates different mechanisms of endothelial cell death. *Cell Tissue Res* 306:409–16

Caplan LR (1994) Hypertensive intracerebral hemorrhage. In: *Intracerebral Hemorrhage* (Kase CR, Caplan LR, eds), Boston, MA: Butterworth-Heinemann, 99–116

Chu Y, Heistad DD, Knudtson KL, Lamping KG, Faraci FM (2002) Quantification of mRNA for endothelial NO synthase in mouse blood vessels by real-time polymerase chain reaction. *Arterioscler Thromb Vasc Biol* 22:611–6

Cunningham LA, Wetzel M, Rosenberg GA (2005) Multiple roles for MMPs and TIMPs in cerebral ischemia. *Glia* 50:329–39

Didion SP, Faraci FM (2003) Angiotensin II produces superoxide-mediated impairment of endothelial function in cerebral arterioles. *Stroke* 34:2038–42

Didion SP, Ryan MJ, Baumbach GL, Sigmund CD, Faraci FM (2002) Superoxide contributes to vascular dysfunction in mice that express human renin and angiotensinogen. *Am J Physiol Heart Circ Physiol* 283:H1569–76

Dong J, Sulik KK, Chen SY (2008) Nrf2-mediated transcriptional induction of antioxidant response in mouse embryos exposed to ethanol *in vivo*: implications for the prevention of fetal alcohol spectrum disorders. *Antioxid Redox Signal* 10:2023–33

Fukai T, Siegfried MR, Fukai-Ushio M, Griendling KK, Harrison DG (1999) Modulation of extracellular superoxide dismutase expression by angiotensin II and hypertension. *Circ Res* 85:23–8

Garcia JH, Wagner S, Liu KF, Hu XJ (1995) Neurological deficit and extent of neuronal necrosis attributable to middle cerebral artery occlusion in rats. *Stroke* 26:627–35

Gasche Y, Copin JC, Sugawara T, Fujimura M, Chan PH (2001) Matrix metalloproteinase inhibition prevents oxidative stress-associated blood–brain barrier disruption after transient focal cerebral ischemia. *J Cereb Blood Flow Metab* 21:1393–400

Grossetete M, Rosenberg GA (2008) Matrix metalloproteinase inhibition facilitates cell death in intracerebral hemorrhage in mouse. *J Cereb Blood Flow Metab* 28:752–63

Heistad DD (2006) Oxidative stress and vascular disease. *Arterioscler Thromb Vasc Biol* 26:689–95

Iida S, Baumbach GL, Lavoie JL, Faraci FM, Sigmund CD, Heistad DD (2005) Spontaneous stroke in a genetic model of hypertensive mice. *Stroke* 36:1253–8

Immenschuh S, Ramadori G (2000) Gene regulation of heme oxygenase-1 as a therapeutic target. *Biochem Pharmacol* 60:1121–8

Inaba S, Iwai M, Furuno M, Tomono Y, Kanno H, Senba I, Okayama H, Mogi M, Higaki J, Horiuchi M (2009) Continuous activation of renin–angiotensin system impairs cognitive function in renin/angiotensinogen transgenic mice. *Hypertension* 53:356–62

Infanger DW, Sharma RV, Davisson RL (2006) NADPH oxidases of the brain: distribution, regulation, and function. *Antioxid Redox Signal* 8:1583–96

Kurtz TW, Griffin KA, Bidani AK, Davisson RL, Hall JE, Subcommittee of Professional and Public Education of the American Heart Association (2005) Recommenda-

tions for blood pressure measurement in humans and experimental animals. Part 2: blood pressure measurement in experimental animals: a statement for professionals from the Subcommittee of Professional and Public Education of the American Heart Association council on high blood pressure research. *Hypertension* 45:299–310

Laursen JB, Rajagopalan S, Galis Z, Tarpey M, Freeman BA, Harrison DG (1997) Role of superoxide in angiotensin II-induced but not catecholamine-induced hypertension. *Circulation* 95:588–93

Liu KJ, Rosenberg GA (2005) Matrix metalloproteinases and free radicals in cerebral ischemia. *Free Radic Biol Med* 39:71–80

MacLellan CL, Silasi G, Poon CC, Edmundson CL, Buist R, Peeling J, Colbourne F (2008) Intracerebral hemorrhage models in rat: comparing collagenase to blood infusion. *J Cereb Blood Flow Metab* 28:516–25

Matsuno K, Yamada H, Iwata K, Jin D, Katsuyama M, Matsuki M, Takai S, Yamanishi K, Miyazaki M, Matsubara H, Yabe-Nishimura C (2005) Nox1 is involved in angiotensin II-mediated hypertension: a study in Nox1-deficient mice. *Circulation* 112:2677–85

Metoki H, Ohkubo T, Kikuya M, Asayama K, Obara T, Hashimoto J, Totune K, Hoshi H, Satoh H, Imai Y (2006) Prognostic significance for stroke of a morning pressor surge and a nocturnal blood pressure decline. The Ohasama Study. *Hypertension* 47:149–54

NINDS ICH Workshop Participants (2005) Priorities for clinical research in intracerebral hemorrhage: report from a National Institute of Neurological Disorders and Stroke workshop. *Stroke* 36:e23–41

Paxinos G, Franklin KBJ (eds) (2000) *The Mouse Brain in Stereotaxic Coordinates*. 2nd ed. London, UK: Academic Press

Poulet P, Gentile MT, Vecchione C, Distaso M, Aretini A, Fratta L, Russo G, Echart C, Maffei A, De Simoni MG, Lembo G (2006) Acute hypertension induces oxidative stress in brain tissues. *J Cereb Blood Flow Metab* 26:253–62

Rajagopalan S, Meng XP, Ramasamy S, Harrison DG, Galis ZS (1996) Reactive oxygen species produced by macrophage-derived foam cells regulate the activity of vascular matrix metalloproteinases *in vitro*: implications for atherosclerotic plaque stability. *J Clin Invest* 98:2572–9

Rosenberg GA, Navratil M, Barone F, Feuerstein G (1996) Proteolytic cascade enzymes increase in focal cerebral ischemia in rat. *J Cereb Blood Flow Metab* 16:360–6

Sadoshima S, Busija D, Brody M, Heistad DD (1981) Sympathetic nerves protect against stroke in stroke-prone hypertensive rats. *Hypertension* 3:I124–7

Shin CY, Lee WJ, Choi JW, Choi MS, Ryu JR, Oh SJ, Cheong JH, Choi EY, Ko KH (2007) Down-regulation of matrix metalloproteinase-9 expression by nitric oxide in lipopolysaccharide-stimulated rat primary astrocytes. *Nitric Oxide* 16:425–32

Ukeda H, Kawana D, Maeda S, Sawamura M (1999) Spectrophotometric assay for superoxide dismutase based on the reduction of highly water-soluble tetrazolium salts by xanthine–xanthine oxide. *Biosci Biotechnol Biochem* 63:485–8

van Wart HE, Birkedal-Hansen H (1990) The cysteine switch: a principle of regulation of metalloproteinase activity with potential applicability to the entire matrix metalloproteinase gene family. *Proc Natl Acad Sci USA* 87:5578–82

Vaughan CJ, Delanty N (2000) Hypertensive emergencies. *Lancet* 356:411–7

Wakisaka Y, Miller JD, Chu Y, Baumbach GL, Wilson S, Faraci FM, Sigmund CD, Heistad DD (2008) Oxidative stress through activation of NAD(P)H oxidase in hypertensive mice with spontaneous intracranial hemorrhage. *J Cereb Blood Flow Metab* 28:1175–85

Woessner Jr JF (1991) Matrix metalloproteinases and their inhibitors in connective tissue remodeling. *FASEB J* 5:2145–54

Xi G, Keep RF, Hoff JT (2006) Mechanisms of brain injury after intracerebral hemorrhage. *Lancet Neurol* 5:53–63

Yang H, Shi M, VanRemmen H, Chen X, Vijg J, Richardson A, Guo Z (2003) Reduction of pressor response to vasoconstrictor agents by overexpression of catalase in mice. *Am J Hypertens* 16:1–5

Yang Y, Estrada EY, Thompson JF, Liu W, Rosenberg GA (2007) Matrix metalloproteinase-mediated disruption of tight junction proteins in cerebral vessels is reversed by synthetic matrix metalloproteinase inhibitor in focal ischemia in rat. *J Cereb Blood Flow Metab* 27:697–709

Zhao BQ, Tejima E, Lo EH (2007) Neurovascular proteases in brain injury, hemorrhage and remodeling after stroke. *Stroke* 38:748–52